HHS Public Access

Author manuscript

Behav Brain Res. Author manuscript; available in PMC 2018 January 01.

Published in final edited form as:

Behav Brain Res. 2017 January 1; 316: 145–151. doi:10.1016/j.bbr.2016.09.007.

ChAT-positive neurons participate in subventricular zone neurogenesis after middle cerebral artery occlusion in mice

Jianping Wang[#a,*], **Xiaojie Fu**[#a], **Di Zhang**[a], **Lie Yu**[a], **Nan Li**[a], **Zhengfang Lu**[a], **Yufeng Gao**[a], **Menghan Wang**[a], **Xi Liu**[a], **Chenguang Zhou**[a], **Wei Han**[a], **Bo Yan**[b], and **Jian Wang**[a,c,*]

[a]Department of Neurology, The Fifth Affiliated Hospital of Zhengzhou University, Zhengzhou 450052, Henan, China

[b]Department of Radiology, The Fourth Affiliated Hospital of Zhengzhou University, Zhengzhou 450052, Henan, China

[c]Department of Anesthesiology/Critical Care Medicine, Johns Hopkins University, School of Medicine, Baltimore, MD, USA.

[#] These authors contributed equally to this work.

Abstract

The mechanisms of post-stroke neurogenesis in the subventricular zone (SVZ) are unclear. However, neural stem cell-intrinsic and neurogenic niche mechanisms, as well as neurotransmitters, have been shown to play important roles in SVZ neurogenesis. Recently, a previously unknown population of choline acetyltransferase $(ChAT)^+$ neurons residing in rodent SVZ were identified to have direct control over neural stem cell proliferation by indirectly activating fibroblast growth factor receptor (FGFR). This finding revealed possible neuronal control over SVZ neurogenesis. In this study, we assessed whether these $ChAT^+$ neurons also participate in stroke-induced neurogenesis. We used a permanent middle cerebral artery occlusion (MCAO) model produced by transcranial electrocoagulation in mice, atropine (muscarinic cholinergic receptor [mAchR] antagonist), and donepezil (acetylcholinesterase inhibitor) to investigate the role of $ChAT^+$ neurons in stroke-induced neurogenesis. We found that mAchRs, phosphorylated protein kinase C (p-PKC), and p-38 levels in the SVZ were upregulated in mice on day 7 after MCAO. MCAO also significantly increased the number of BrdU/doublecortin-positive cells and protein levels of phosphorylated–neural cell adhesion molecule and mammalian achaete scute homolog-1. FGFR was activated in the SVZ, and doublecortin-positive cells increased in the peri-infarction region. These post-stroke neurogenic effects were enhanced by donepezil and partially decreased by atropine. Neither atropine nor donepezil affected peri-infarct microglial activation or serum concentrations of TNF-α, IFN-γ, or TGF-β on day 7 after MCAO. We

[*]Address correspondence to: Jianping Wang, MD, PhD, Department of Neurology, The Fifth Affiliated Hospital of Zhengzhou University, Zhengzhou 450052, Henan, China (Phone: 011-86-371-68322417; Fax: 86-371-66965783; wjpwfy666@126.com) Or: Jian Wang, MD, PhD, Department of Anesthesiology/Critical Care Medicine, Johns Hopkins University, School of Medicine, Baltimore, MD, USA. (Phone: 443-287-5490; Fax: 410-502-5177; jwang79@jhmi.edu).

conclude that ChAT$^+$ neurons in the SVZ may participate in stroke-induced neurogenesis, suggesting a new mechanism for neurogenesis after stroke.

Keywords

ChAT+ neurons; stroke; neurogenesis; subventricular zone

1. Introduction

Neurogenesis continues throughout the life of adult mammals and has been clearly demonstrated at two locations: the subventricular zone (SVZ) of the lateral ventricles and the subgranular zone of the dentate gyrus in the hippocampus [1]. Neural stem cells (NSCs) residing in the SVZ give rise to neuroblasts that migrate to the olfactory bulb in mammals [2]. The fate of such neuroblasts is unknown because the density of neuroblasts in human SVZ is similar to that in the subgranular zone, but limited postnatal neurogenesis is observed in the human olfactory bulb [3]. Recent research has shown that NSCs in the human SVZ can develop into new neurons that integrate into the striatum [4], suggesting that neurogenesis in the SVZ may be utilized therapeutically in neurologic diseases.

The mechanism of postnatal and adult neurogenesis in the SVZ is unclear. Most research shows that it is controlled by an intrinsic mechanism in which NSCs interact with extracellular and niche-driven cues [1, 5, 6]. However, recent studies showed that neurotransmitters can also influence NSC proliferation [7, 8], indicating possibilities for higher level inputs during SVZ neurogenesis. Recently, Paez-Gonzalez and colleagues [9] identified a previously unknown population of choline acetyltransferase (ChAT)-positive (+) neurons residing in the rodent SVZ neurogenic niche that can exert activity-dependent control over the proliferative activity and neurogenic response of NSCs in the SVZ. They described a new mechanism by which activity of neural networks can be translated into NSC-dependent plasticity. However, when and how this system is used to regulate neurogenesis remains unknown.

Ischemic stroke induces proliferation of NSCs in the SVZ and attracts newborn neurons to the injury zone [10]. Additionally, treatments that increase SVZ neurogenesis have been correlated with enhanced functional recovery [11, 12]. However, the mechanism of stroke-induced neurogenesis is not clear. In this study, we investigated whether the newly found ChAT$^+$ neurons that reside in the SVZ niche also participate in stroke-induced neurogenesis.

2. Materials and methods

2.1. Animals and ethics statement

Male C57BL/6 mice (25-30 g, 12-14 weeks old) were purchased from the Animal Experimental Center of Zhengzhou University. All mice were housed in plastic cages (8 per cage) with free access to food and water and were maintained at a constant temperature of 22±1°C. All protocols were approved by the Animal Care and Use Committee of Zhengzhou University. All efforts were made to minimize the number of animals used and their suffering.

2.2. Middle cerebral artery occlusion model

Mice were subjected to the permanent middle cerebral artery occlusion (MCAO) model of ischemic stroke by transcranial electrocoagulation as previously described [13]. Briefly, we anesthetized mice with an intraperitoneal injection of 4% chloral hydrate (400 mg/kg) and made a 1-cm skin incision between the left ear and eye. We carefully detached the temporal muscle from the skull by using bipolar electrocoagulation forceps at 12 W. We identified the MCA below the skull in the rostral part of the temporal area, dorsal to the retro-orbital sinus, and thinned out the bone with a drill directly above the MCA branch. The arteries proximal and distal to the bifurcation were coagulated with the bipolar electrocoagulation forceps at 7 W. We then replaced the temporal muscle, sutured the wound, and placed the animal in a nursing box at 32°C to recover from the anesthesia. The sham procedure was performed as described above without coagulation of the MCA.

2.3. Treatment and groups

We randomly assigned the mice to six groups [14]: sham-operated mice treated with vehicle (Sham+vehicle, n=24), MCAO-operated mice treated with vehicle (MCAO+vehicle, n=32), sham-operated mice treated with atropine (Sham+atropine, n=16), MCAO mice treated with atropine (MCAO+atropine, n=24), sham-operated mice treated with donepezil (Sham +donepezil, n=16), and MCAO mice treated with donepezil (MCAO+donepezil, n=24). Donepezil (selective acetylcholinesterase [AchE] inhibitor, 5 mg/kg/day, Abcam, Cambridge, MA, USA) was dissolved in drinking water and administrated orally on days 1, 3, 5, and 7 after MCAO or sham surgery [15]. Atropine (competitive inhibitor of muscarinic acetylcholine receptors [mAchRs], 5 mg/kg/day, Abcam) was administrated by intragastric delivery on days 1, 3, 5, and 7 after MCAO or sham surgery [15]. All mice except those prepared for neurologic function assessment received intraperitoneal injection of 5-bromo-2’-deoxyuridine (BrdU; 50 mg/kg, Sigma-Aldrich, St Louis, MO, USA) once daily for 7 days.

2.4. Neurologic function assessment

We used neurologic deficit scoring and the cylinder test to assess neurologic deficits of the mice as previously described [13, 16]. The assessments were conducted on days 1, 7, 14, and 28 after the MCAO procedure (n=10 per group). Neurologic deficits were scored by using a 5-point scale [17]: 0 = no neurologic deficit, 1 = failure to fully extend right forepaw, 2 = circling to the right, 3 = falling to the right, and 4 = no spontaneous walking and depressed level of consciousness. For the cylinder test [13], mice were placed in a transparent acrylic cylinder (diameter: 8 cm, height: 25 cm), and their forelimb activity as they reared up against the wall was recorded. Independent forelimb use was recorded according to the following standards: 1) contact of the cylinder wall with one forelimb during full rear and 2) landing with only one forelimb on the floor after full rear. An investigator blinded to the treatment groups recorded the number of impaired right and non-impaired left forelimb contacts, with a total of 20 contacts for each mouse.

2.5. Infarct volume analysis

On day 7 after MCAO, we sacrificed eight mice per group to measure infarct volume with Nessl staining as previously described [18]. Briefly, after being deeply anesthetized with 10% chloral hydrate, the mice were transcardially perfused with 0.01 mol/L phosphate-buffered saline (PBS; pH 7.4) followed by 4% paraformaldehyde in 0.01 mol/L PBS (pH 7.4). Brains were removed, post-fixed in 4% paraformaldehyde overnight, and stored in 30% sucrose/0.01 mol/L PBS until the tissue sank. Then the brain was serially cut into 20-μm-thick floating sections every 480 μm by cryoultramicrotomy (CM1100, Leica Biosystems, Germany) and stored in antifreeze buffer in 24-well plates at −20°C for future use. The serial brain sections were placed on slides for Nessl staining according to the standard protocol of the manufacturer (Beyotime Institute of Biotechnology, China). All slides were viewed and photographed under a microscope (Zeiss Stemi 2000-CS, Zeiss, Germany). The infarct volume was analyzed by the Swanson method [19] to correct for edema: Ischemic area = (cortex area of contralateral side) – (non-ischemic cortex area of ipsilateral side).

2.6. Immunofluorescence analysis

The brain sections used for infarct volume analysis were also used for immunofluorescence analysis [14]. Briefly, seven or eight sections of each mouse were washed three times for 5 min in 0.01 mol/L PBS. The sections used for BrdU detection were incubated in 2 mol/L HCl for 30 min followed by 0.1 mol/L sodium borate buffer (pH 8.5) for 10 min. After incubation with 1% bovine serum albumin in PBST (PBS + 0.25% Triton X-100) for 30 min, the sections were incubated with sheep anti-ChAT antibody (1:1000, Abcam), goat anti-doublecortin (DCX) antibody (1:200, Santa Cruz Biotechnology, Dallas, TX, USA), rat anti-BrdU antibody (1:250, Abcam), or rabbit anti-Iba1 antibody (1:500, Abcam) for 1 h at room temperature or overnight at −4°C. Then they were washed three times with 0.01 mol/L PBS and incubated with appropriate secondary antibody for 1 h at room temperature. All sections were finally washed three times with 0.01 mol/L PBS for 5 min and mounted on cover slips with a drop of mounting medium containing 1.5 μg/mL 4',6-diamidino-2-phenylindole (DAPI) (Santa Cruz). Brain sections that contained SVZ from one brain serial section were chosen for quantification of SVZ $ChAT^+$ cells and SVZ $BrdU/DCX^+$ cells. The $ChAT^+$ or $BrdU/DCX^+$ cells within the SVZ of the ischemic hemisphere were expressed as average cell numbers per section. For each section that contained brain infarction, we randomly chose three 20X fields in peri-infarction zones to quantify DCX^+ cells and/or $Iba1^+$ cells. Reactive microglia were characterized as $Iba1^+$ cells with a rod-like, spherical, or amoeboid appearance, and a cell body more than 10 μm in diameter that had short, thick processes and intense immunoreactivity. The resting microglia were characterized by a small cell body that had long processes and weak immunoreactivity [20, 21]. Investigators blinded to the treatment groups conducted all observations and quantifications using a fluorescence microscope (ZEISS ScopeA1, ZEISS, Germany).

2.7. Western blot analysis

We sacrificed eight mice per group for Western blot analysis to determine protein level changes in the SVZ on day 7 after the MCAO procedure [22]. Mice were deeply anesthetized, and SVZ tissue (from the ipsilateral hemisphere of ischemic mice) was quickly

dissected from the frontal slice extending between the crossing of the anterior commissure and the rostral opening of the third ventricle [23]. The SVZ tissue was homogenized in radioimmunoprecipitation assay lysis buffer containing a protease/phosphatase inhibitor mixture (Beyotime Institute of Biotechnology). The sample was centrifuged for 2 min at 14,000 × *g* and 4°C. Supernatants were separated by 12% sodium dodecyl sulfate-polyacrylamide gel electrophoresis and transferred onto polyvinylidene fluoride membranes (PVDF membrane, Millipore, Billerica, MA, USA). A prestained protein marker (Sangon Biotech, Shanghai, China) was used during the separation process. Membranes were blocked with 5% nonfat milk (Sigma-Aldrich) for 1 h at room temperature and then incubated with primary antibody against ChAT (1:50, Abcam), vesicle acetylcholine transporter (VAChT; 1:150, Santa Cruz), AchE (1:200, Santa Cruz), mAchR (1:300, Argene, France), p-PKC (1:150, Santa Cruz), p-38 (1:200, Santa Cruz), phosphorylated–neural cell adhesion molecule (PSA-NCAM; 1:300, Millipore), mammalian achaete scute homolog-1 (mash1; 1:300, Santa Cruz), phosphorylated fibroblast growth factor receptor (p-FGFR; 1:800, Cell Signaling), and glyceraldehyde 3-phosphate dehydrogenase (GAPDH; 1:2000, HangZhou Goodhere Biotechnology, Zhejiang, China). After three washes, membranes were incubated with appropriate horseradish peroxidase (HRP)-conjugated secondary antibodies. Protein bands were visualized by enhanced chemiluminescence detection kit (Beyotime Institute of Biotechnology). An investigator blinded to the animal group quantified the optical density of the protein bands using Gel Analysis V 2.02 software (Clinx Science Instruments).

2.8. ELISA analysis

We collected peripheral blood from the mice used for Western blot analysis to measure serum levels of pro-inflammatory cytokines TNF-α and IFN-γ, as well as anti-inflammatory cytokine TGF-β, using ELISA kits (R&D Systems, USA) [24].

2.9. Statistical analysis

Statistical analysis was carried out with SPSS version 13.0. All results are expressed as mean ± SD. We used repeated measures ANOVA followed by the least significant difference (LSD) test to determine changes in neurologic deficit score and cylinder test function among different groups. We used one-way ANOVA followed by the LSD test to analyze differences of data in the immunofluorescence analysis and Western blot analysis. $p<0.05$ was considered statistically significant.

3. Results

3.1. Effect of MCAO on cholinergic system in SVZ

We found similar numbers of $ChAT^+$ cells in the SVZ of mice from sham+vehicle and MCAO+vehicle groups (Fig. 1A-C). Quantification of Western blot analysis showed that expression levels of ChAT, VAChT, and AchE in the SVZ were lower in MCAO mice than in sham-operated mice on day 7 after the procedure (Fig. 1D-G). However, the mAchR level in MCAO mice was significantly higher than that in sham-operated mice (Fig. 1H, I). The MCAO procedure also increased the expression of p-APK and p-38 in the SVZ compared to that in the sham groups (Fig. 2H, J, K). These proteins are downstream of the mAchR signaling pathway.

3.2. Infarct volume and neurologic assessment

We found that neither atropine nor donepezil affected the infarct volume of MCAO mice on day 7 after surgery (Fig. 2A and B). However, donepezil-treated MCAO mice had lower neurologic deficit scores and exhibited greater right-forelimb use than did vehicle- or atropine-treated mice during the 28-day experiment (Fig. 2C and D). Although mice that received atropine had a lower average percentage of right-forelimb use than the vehicle group at each time point, no significant differences were found between the two groups (Fig. 2D).

3.3. Function of ChAT$^+$ neurons in stroke-induced neurogenesis

Immunofluorescence analysis showed that MCAO mice had more BrdU/DCX$^+$ cells in the SVZ and more DCX$^+$ cells in the peri-infarction region than did the sham group on day 7 after surgery (Fig. 3A-D). This stroke-induced neurogenesis was decreased by atropine administration and enhanced by donepezil (Fig. 3A-D). Western blot analyses of SVZ lysates showed that the levels of PSA-NCAM, mash1, and p-FGFR, which participate in the activation, proliferation, and differentiation of NSCs [4], were significantly higher at 7 days after MCAO than at 7 days after the sham procedure (Fig. 3E-H). Activation of the cholinergic system by donepezil significantly enhanced the stroke-induced upregulation of PSA-NCAM, mash1, and p-FGFR levels (Fig. 3E-H). In the sham groups, donepezil also increased the levels of these three proteins compared to levels in the vehicle- and atropine-treated groups (Fig. 3E-H). Inhibition of mAchR by atropine significantly decreased mash1 level, but had no effect on PSA-NCAM and p-FGFR levels in the MCAO mice compared to those in the vehicle-treated mice.

3.4. Effect of drug treatment on SVZ niche and FGFR activation

SVZ neurogenesis is greatly affected by the local microenvironment [1]. To exclude the inflammatory changes caused by atropine and donepezil administration, we assessed the number of reactive microglia in the peri-infarction zone, the serum level of pro-inflammatory cytokines TNF-α and IFN-γ, and the serum level of anti-inflammatory cytokine TGF-β on day 7 after MCAO or sham surgery. Quantification of immunofluorescence showed that mice that underwent MCAO had similar numbers of reactive microglia in the peri-infarction region, regardless of treatment (Fig. 4.A-C). ELISA showed that all six groups had similar serum levels of TNF-α, IFN-γ, and TGF-β on day 7 after MCAO (Fig. 4D-F).

4. Discussion

Our study showed that the cholinergic system in the SVZ is activated after stroke and participates in stroke-induced neurogenesis, probably through the FGFR signaling pathway. These results suggest that the newly found ChAT$^+$ neurons in the SVZ may play an important neurogenic role after stroke.

The mechanism of NSC proliferation in the SVZ is complex; it was reported to be controlled by cell-intrinsic molecular pathways and significantly affected by the NSC microenvironment [1, 12, 25]. Neurotransmitters can also influence SVZ neurogenesis [26].

The SVZ neurogenic niches were found to be overlapped by dense dopaminergic projections with dense serotonergic projections (originating from a small group of neurons in the raphe) [7, 26]. Such findings suggest that cooperation of neuronal systems may contribute to establishment of the SVZ microenvironment and influence the proliferation of NSCs, which contribute to learning/exercise-induced neurogenesis [27, 28]. Paez-Gonzalez *et al.* [9] recently identified a set of $ChAT^+$ neurons in the mouse SVZ neurogenic niche that can exert activity-dependent control over the proliferative activity and neurogenic response of NSCs via FGFR activation. This finding suggests that such $ChAT^+$ neurons may be the terminal station of the whole neurogenic neural circuit. However, whether this system also functions after stroke remains unknown.

In this study, we first assessed the effect of MCAO on the cholinergic system in the SVZ. We found no differences in the number of $ChAT^+$ cells between sham and MCAO mice. However, MCAO significantly reduced the protein level of ChAT and VAChT in the SVZ, possibly as a result of severe ischemic lesions [29]; however, the low level of AchE and upregulation of mAchRs, p-PKC, and p-38 indicated that the cholinergic system was activated after MCAO. We then observed more proliferative neuroblasts ($BrdU^+$ and DCX^+ cells) and higher levels of PSA-NCAM and mash1 protein in the SVZ after stroke. These results show that activation of the cholinergic system ($ChAT^+$ neurons) may participate in stroke-induced neurogenesis.

To verify the relationship between $ChAT^+$ neurons and stroke-induced SVZ neurogenesis, we used atropine and donepezil to inhibit or activate the cholinergic system. Atropine is a competitive antagonist of mAchRs, and donepezil is a reversible AchE inhibitor. Both drugs can easily cross the blood-brain barrier [30]. We found that donepezil improved the performance of MCAO mice in the neurologic deficit score and cylinder tests. Although atropine-treated mice used their right forelimb less than the vehicle group did at each time point, no significant difference was noted between the two groups. In addition, SVZ neurogenesis was significantly enhanced by the administration of donepezil, but partially decreased by atropine, as evidenced by $BrdU^+$ and DCX^+ cells and the levels of PSA-NCAM and mash1 protein. These data indicate that activation of the cholinergic system, not only the mAchR signaling pathway, in the SVZ after stroke participates in stroke-induced neurogenesis.

Considering that changes in infarct volume or microenvironment by drug (atropine or donepezil) intake may influence NSC proliferation, we assessed infarct volume, reactive microglia in the peri-infarction region, and serum levels of TNF-α, IFN-γ, and TGF-β on day 7 after MCAO in each group. We found that neither atropine nor donepezil affected the infarct volume, the number of reactive microglia in the peri-infarction region, or the serum levels of the three cytokines, further supporting the cholinergic system's role in neurogenesis after stroke. It has been reported that $ChAT^+$ neurons may promote SVZ NSC proliferation by indirect activation of the FGF pathway [9], which has been shown to be vital for neurogenesis [31]. We also found activation of FGFR after stroke. This activation was further elevated in the donepezil-treated mice, indicating that $ChAT^+$ neurons may increase SVZ neurogenesis via the FGFR signaling pathway.

In conclusion, we showed that the newly found ChAT$^+$ neurons in the SVZ may also participate in stroke-induced neurogenesis. Protection and upregulation of ChAT$^+$ neuron activity may promote neurogenesis after stroke. However, the relationship between ChAT$^+$ neurons and other neurogenic neural circuits remains unknown, and the downstream molecular pathways of ChAT$^+$ neuron-promoted neurogenesis need additional research.

Acknowledgements

This work was supported by grants from NSFC (81271284, 81571137), the American Heart Association (13GRNT15730001), and the National Institutes of Health (R01NS078026, R01AT007317). We thank Yoyo Wang and Claire Levine for assistance with this manuscript.

References

1. Zhao C, Deng W, Gage FH. Mechanisms and functional implications of adult neurogenesis. Cell. 2008; 132(4):645–60. [PubMed: 18295581]
2. Ming G-L, Song H. Adult neurogenesis in the mammalian brain: significant answers and significant questions. Neuron. 2011; 70(4):687–702. [PubMed: 21609825]
3. Bergmann O, Liebl J, Bernard S, Alkass K, Yeung MSY, Steier P, Kutschera W, Johnson L, Landen M, Druid H, Spalding KL, Frisen J. The age of olfactory bulb neurons in humans. Neuron. 2012; 74(4):634–9. [PubMed: 22632721]
4. Ernst A, Alkass K, Bernard S, Salehpour M, Perl S, Tisdale J, Possnert G, Druid H, Frisen J. Neurogenesis in the striatum of the adult human brain. Cell. 2014; 156(5):1072–83. [PubMed: 24561062]
5. Zhang RL, Chopp M, Roberts C, Jia L, Wei M, Lu M, Wang X, Pourabdollah S, Zhang ZG. Ascl1 lineage cells contribute to ischemia-induced neurogenesis and oligodendrogenesis. Journal of cerebral blood flow and metabolism : official journal of the International Society of Cerebral Blood Flow and Metabolism. 2011; 31(2):614–25.
6. Ottone C, Krusche B, Whitby A, Clements M, Quadrato G, Pitulescu ME, Adams RH, Parrinello S. Direct cell-cell contact with the vascular niche maintains quiescent neural stem cells. Nature cell biology. 2014; 16(11):1045–56. [PubMed: 25283993]
7. Tong CK, Chen J, Cebrian-Silla A, Mirzadeh Z, Obernier K, Guinto CD, Tecott LH, Garcia-Verdugo JM, Kriegstein A, Alvarez-Buylla A. Axonal control of the adult neural stem cell niche. Cell stem cell. 2014; 14(4):500–11. [PubMed: 24561083]
8. Young SZ, Taylor MM, Bordey A. Neurotransmitters couple brain activity to subventricular zone neurogenesis. The European journal of neuroscience. 2011; 33(6):1123–32. [PubMed: 21395856]
9. Paez-Gonzalez P, Asrican B, Rodriguez E, Kuo CT. Identification of distinct ChAT$^+$ neurons and activity-dependent control of postnatal SVZ neurogenesis. Nature neuroscience. 2014; 17(7):934–42. [PubMed: 24880216]
10. Kreuzberg M, Kanov E, Timofeev O, Schwaninger M, Monyer H, Khodosevich K. Increased subventricular zone-derived cortical neurogenesis after ischemic lesion. Experimental neurology. 2010; 226(1):90–9. [PubMed: 20713052]
11. Li J, Siegel M, Yuan M, Zeng Z, Finnucan L, Persky R, Hurn PD, McCullough LD. Estrogen enhances neurogenesis and behavioral recovery after stroke. J Cereb Blood Flow Metab. 2011; 31(2):413–25. [PubMed: 20940729]
12. Maya-Espinosa G, Collazo-Navarrete O, Millan-Aldaco D, Palomero-Rivero M, Guerrero-Flores G, Drucker-Colin R, Covarrubias L, Guerra-Crespo M. Mouse embryonic stem cell-derived cells reveal niches that support neuronal differentiation in the adult rat brain. Stem Cells. 2014
13. Llovera G, Roth S, Plesnila N, Veltkamp R, Liesz A. Modeling stroke in mice: permanent coagulation of the distal middle cerebral artery. J Vis Exp. 2014; 89:e51729. [PubMed: 25145316]
14. Han X, Lan X, Li Q, Gao Y, Zhu W, Cheng T, Maruyama T, Wang J. Inhibition of prostaglandin E2 receptor EP3 mitigates thrombin-induced brain injury. J Cereb Blood Flow Metab. 2016; 36(6): 1059–74. [PubMed: 26661165]

15. Kakinuma Y, Furihata M, Akiyama T, Arikawa M, Handa T, Katare RG, Sato T. Donepezil, an acetylcholinesterase inhibitor against Alzheimer's dementia, promotes angiogenesis in an ischemic hindlimb model. J Mol Cell Cardiol. 2010; 48(4):680–93. [PubMed: 19962381]
16. Schallert T, Fleming SM, Leasure JL, Tillerson JL, Bland ST. CNS plasticity and assessment of forelimb sensorimotor outcome in unilateral rat models of stroke, cortical ablation, parkinsonism and spinal cord injury. Neuropharmacology. 2000; 39(5):777–87. [PubMed: 10699444]
17. Caltana L, Saez TM, Aronne MP, Brusco A. Cannabinoid receptor type 1 agonist ACEA improves motor recovery and protects neurons in ischemic stroke in mice. J Neurochem. 2015; 135(3):616–29. [PubMed: 26296704]
18. Wu H, Wu T, Hua W, Dong X, Gao Y, Zhao X, Chen W, Cao W, Yang Q, Qi J, Zhou J, Wang J. PGE2 receptor agonist misoprostol protects brain against intracerebral hemorrhage in mice. Neurobiol Aging. 2015; 36(3):1439–50. [PubMed: 25623334]
19. Swanson RA, Morton MT, Tsao-Wu G, Savalos RA, Davidson C, Sharp FR. A semiautomated method for measuring brain infarct volume. Journal of cerebral blood flow and metabolism : official journal of the International Society of Cerebral Blood Flow and Metabolism. 1990; 10(2): 290–3.
20. Wang J, Dore S. Heme oxygenase-1 exacerbates early brain injury after intracerebral haemorrhage. Brain. 2007; 130(Pt 6):1643–52. [PubMed: 17525142]
21. Rogove AD, Siao C, Keyt B, Strickland S, Tsirka SE. Activation of microglia reveals a non-proteolytic cytokine function for tissue plasminogen activator in the central nervous system. J Cell Sci. 1999; 112(Pt 22):4007–16. [PubMed: 10547361]
22. Zhao X, Wu T, Chang CF, Wu H, Han X, Li Q, Gao Y, Hou Z, Maruyama T, Zhang J, Wang J. Toxic role of prostaglandin E2 receptor EP1 after intracerebral hemorrhage in mice. Brain Behav Immun. 2015; 46:293–310. [PubMed: 25697396]
23. Katakowski M, Chen J, Zhang ZG, Santra M, Wang Y, Chopp M. Stroke-induced subventricular zone proliferation is promoted by tumor necrosis factor-alpha-converting enzyme protease activity. J Cereb Blood Flow Metab. 2007; 27(4):669–78. [PubMed: 16926839]
24. Chang CF, Cho S, Wang J. (-)-Epicatechin protects hemorrhagic brain via synergistic Nrf2 pathways. Ann Clin Transl Neurol. 2014; 1(4):258–71. [PubMed: 24741667]
25. Crews L, Patrick C, Adame A, Rockenstein E, Masliah E. Modulation of aberrant CDK5 signaling rescues impaired neurogenesis in models of Alzheimer's disease. Cell Death Dis. 2011; 2:e120. [PubMed: 21368891]
26. Hagg T. Molecular regulation of adult CNS neurogenesis: an integrated view. Trends Neurosci. 2005; 28(11):589–95. [PubMed: 16153715]
27. Merritt JR, Rhodes JS. Mouse genetic differences in voluntary wheel running, adult hippocampal neurogenesis and learning on the multi-strain-adapted plus water maze. Behav Brain Res. 2015; 280:62–71. [PubMed: 25435316]
28. Kondo M, Nakamura Y, Ishida Y, Shimada S. The 5-HT receptor is essential for exercise-induced hippocampal neurogenesis and antidepressant effects. Mol Psychiatry. 2014
29. Nakai M, Akino H, Kaneda T, Matsuta Y, Shiyama R, Tanase K, Ito H, Aoki Y, Oyama N, Miwa Y, Yokoyama O. Acetylcholinesterase inhibitor acting on the brain improves detrusor overactivity caused by cerebral infarction in rats. Neuroscience. 2006; 142(2):475–80. [PubMed: 16905267]
30. Banks WA. Drug delivery to the brain in Alzheimer's disease: consideration of the blood-brain barrier. Adv Drug Deliv Rev. 2012; 64(7):629–39. [PubMed: 22202501]
31. Patel NS, Rhinn M, Semprich CI, Halley PA, Dolle P, Bickmore WA, Storey KG. FGF signalling regulates chromatin organisation during neural differentiation via mechanisms that can be uncoupled from transcription. PLoS genetics. 2013; 9(7):e1003614. [PubMed: 23874217]

Research Highlights

- SVZ choline acetyltransferase $(ChAT)^+$ neurons promote neurogenesis in adult mice.
- SVZ neurogenesis was elevated after middle cerebral artery occlusion (MCAO) in mice.
- The cholinergic system in the SVZ was activated after MACO.
- Post-stroke neurogenesis was enhanced by donepezil and abolished by atropine.
- SVZ $ChAT^+$ neurons may promote neurogenesis via the FGFR signaling pathway.

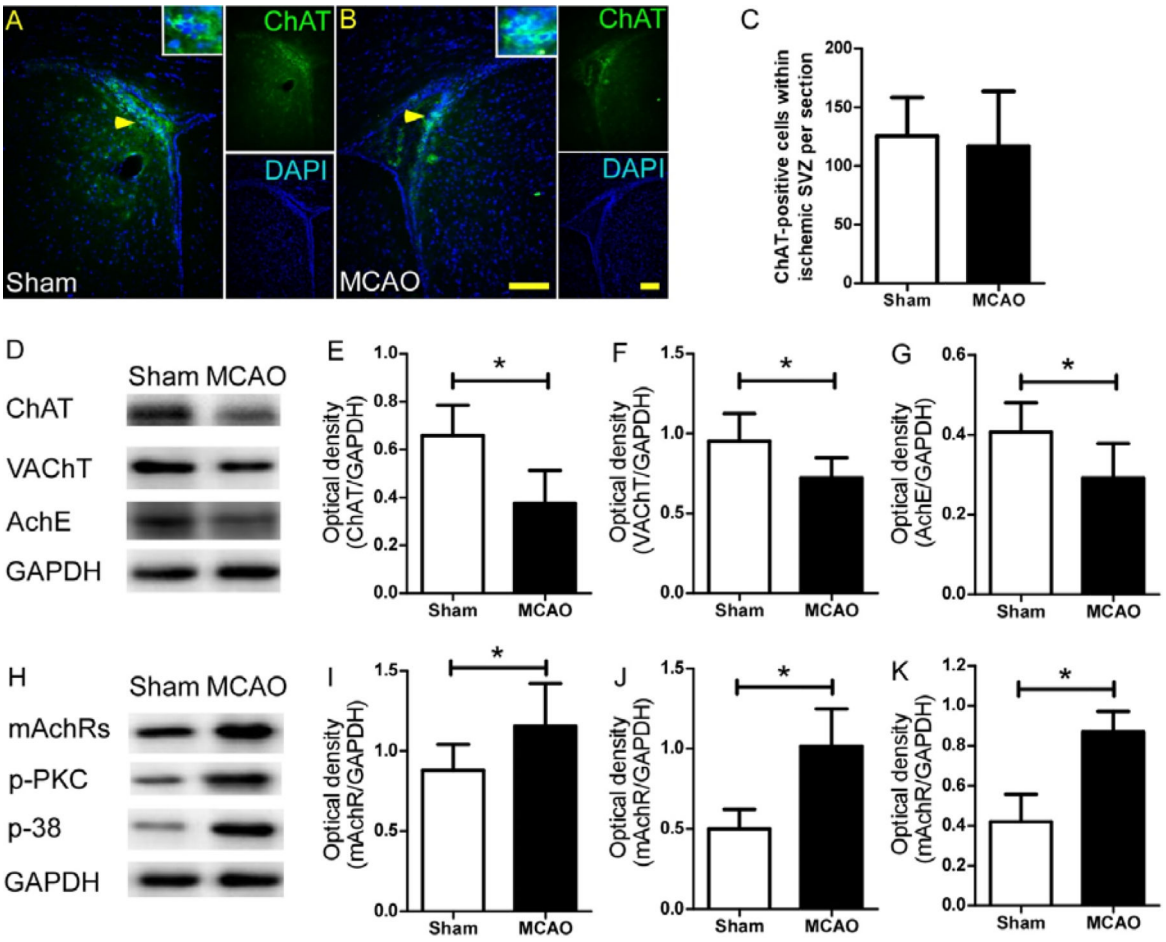

Figure 1.

The cholinergic system in the subventricular zone (SVZ) is activated after stroke. (A and B) Immunofluorescence staining of choline acetyltransferase-positive ($ChAT^+$) cells in the SVZ on day 7 after permanent middle cerebral artery occlusion (MCAO). Scale bar, 50 μm. (C) Quantification showed that MCAO did not affect the number of $ChAT^+$ cells in the SVZ ($p>0.05$, $n=8$/group). (D and H) Western blot analysis of ChAT, VAChT, AchE, mAchR, p-PKC, and p-38 levels in the SVZ on day 7 after MCAO. GAPDH was used as a loading control. (E-G and I-K) Quantification of band densities showed that MCAO significantly decreased the ChAT, VAChT, and AchE levels and elevated the mAchR, p-PKC, and p-38 levels in the SVZ compared to those of sham control mice. *$p<0.05$, $n=8$/group. Values are mean ± SD.

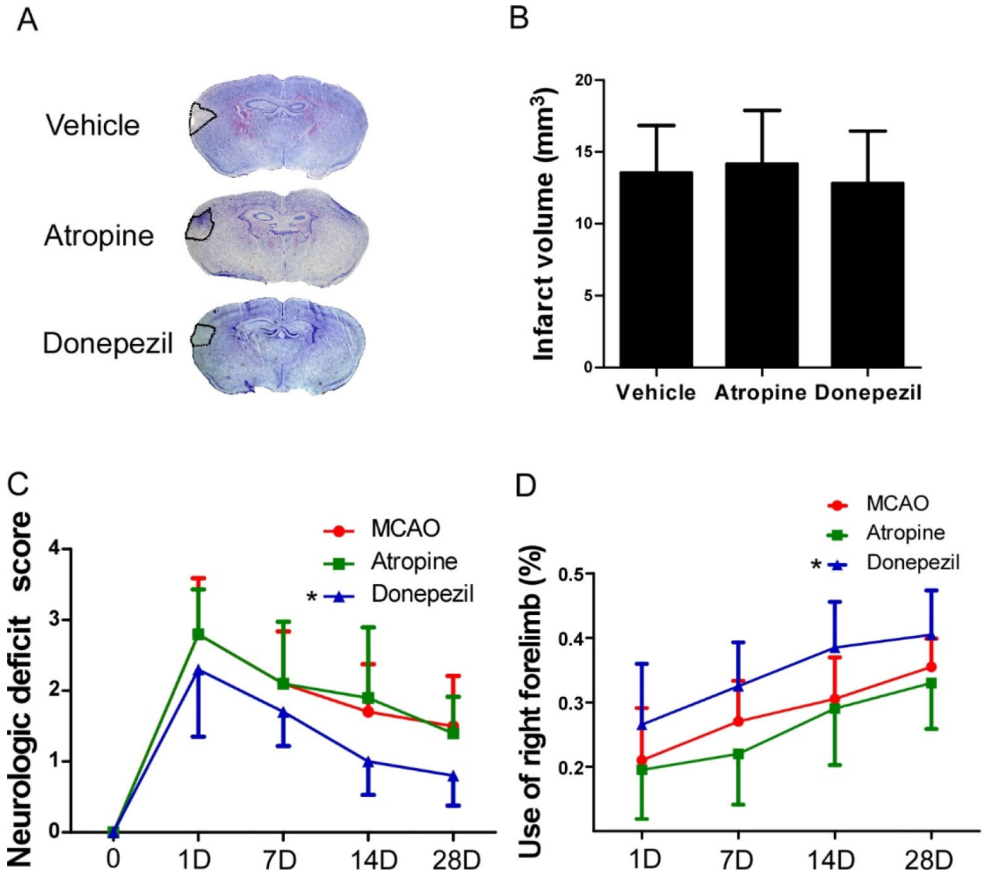

Figure 2.

Infarct volume analysis and neurologic function assessments. (A) Nessl staining of brain sections from vehicle-, atropine-, and donepezil-treated MCAO mice on day 7 after surgery. (B) Quantification showed that neither atropine nor donepezil affected the infarct volume. $p>0.05$, $n=8$/group. (C) Neurologic deficit score showed that donepezil significantly improved the neurologic recovery of MCAO mice. No differences were found between vehicle- and atropine-treated groups. *$p<0.05$ vs. vehicle group, $n=10$/group. (D) Quantification showed that donepezil significantly increased use of the impaired right forelimb of MCAO mice. No differences were found between vehicle- and atropine-treated groups. *$p<0.05$ vs. vehicle group, $n=8$/group. Values are mean ± SD.

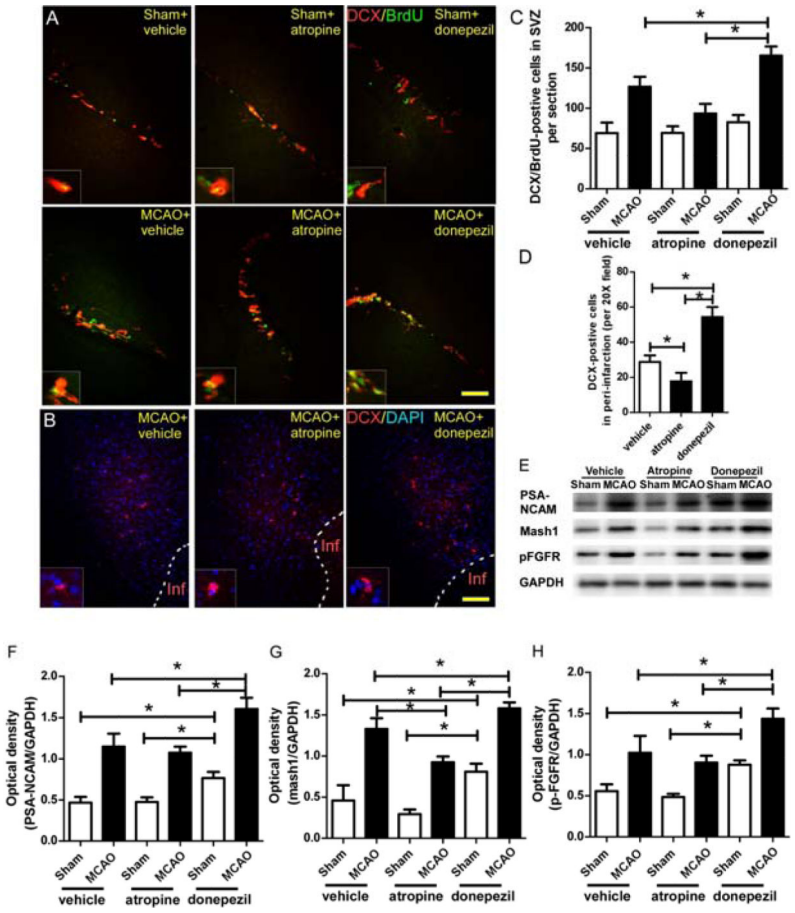

Figure 3.

The cholinergic system (ChAT$^+$ neurons) participates in post-stroke neurogenesis. (A) Immunofluorescence staining of BrdU and DCX in the SVZ of mice on day 7 after MCAO. (B) Immunofluorescence staining of DCX in the peri-infarction region of mice on day 7 after MCAO. (C and D) Quantification showed that activation of the cholinergic system by donepezil significantly increased the number of BrdU/DCX$^+$ cells in the SVZ and the number of DCX$^+$ cells in the peri-infarction region compared with the corresponding numbers in the vehicle-treated MCAO mice; inhibition of mAchRs by atropine significantly reversed these effects. *p<0.05, n=8/group. Values are mean ± SD. (E) Western blot analysis of PSA-NCAM, mash1, and p-FGFR in SVZ on day 7 after MCAO. GAPDH was used as a loading control. (F-H) Quantification of band densities showed that vehicle-treated MCAO mice had higher levels of PSA-NCAM, mash1, and p-FGFR in SVZ than did the sham +vehicle group. Donepezil significantly enhanced this neurogenic effect. Atropine significantly decreased the mash1 level in the SVZ of MCAO mice compared to that of the MCAO+vehicle group. In the sham groups, donepezil also increased the levels of PSA-NCAM, mash1, and p-FGFR compared with levels in the other two sham groups. *p<0.05, n=8/group. Values are mean ± SD.

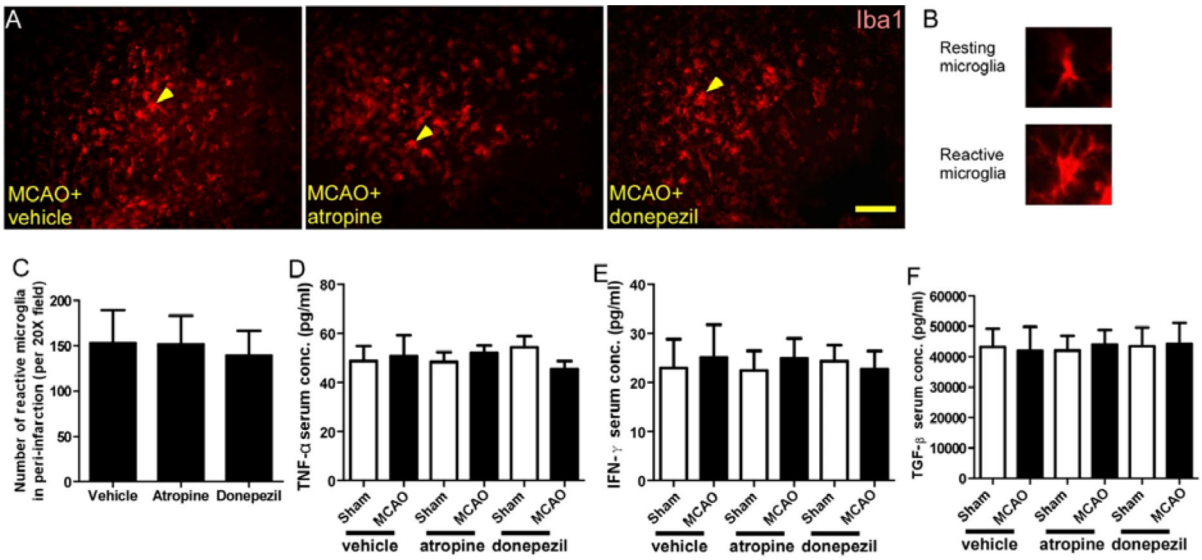

Figure 4.

Atropine and donepezil do not affect inflammation after stroke. (A-B) Immunofluorescence staining of Iba1 in the peri-infarction region of mice on day 7 after MCAO. (C) Quantification showed that neither atropine nor donepezil affected the number of reactive microglia in the peri-infarction region. *$p<0.05$, $n=8$/group. (D-F) ELISA analysis showed that atropine and donepezil had no effect on the serum concentrations of TNF-α, IFN-γ, and TGF-β on day 7 after MCAO. *$p<0.05$, $n=8$/group. Values are mean ± SD.